Characterization of CESR BPMs Using a BPM Test Stand

Jeremy Urban, Nabil Iqbal, Georg Hoffstaetter, and Mike Billing

Laboratory for Elementary Particle Physics,

Cornell University, Ithaca, New York 14853

We built a test stand to investigate the accuracy of the nonlinear model used to simulate the CESR BPM response. A movable wire simulating the beam was used to map the interior of the BPM. Results will be presented which show agreement between this experimental map and the nonlinear map of the BPMs currently in use at CESR, although not all aspects of the response could be completely explained.

I. INTRODUCTION

Accurate beam position measurement The accurate measurement of the position of the beam in a particle accelerator hinges upon a thorough understanding of how a beam position monitor (BPM) responds to different shapes and sizes of charged particle bunches. Unfortunately, once the BPM has been mounted in a particle accelerator, the electronics which process the detector response and the inability to completely control the source which drives the detector, the bunches themselves, complicate the task of determining the true response of the BPM. A BPM test stand was proposed to allow reproducible control of the input and output of the BPM permitting a characterization of BPMs before installation in the Cornell Electron Storage Ring (CESR).

Ensuring an impedance matched test stand allows this test stand to be used in the future for high frequency measurements which would be necessary to investigate the bunch-length dependence of button response models, as well as for the testing and characterization of suitable BPM designs for the Energy Recovery Linac (ERL) at CESR. The need for an impedance matched test stand precluded the use of a translation stage as traditionally used for BPM mapping experiments [1].

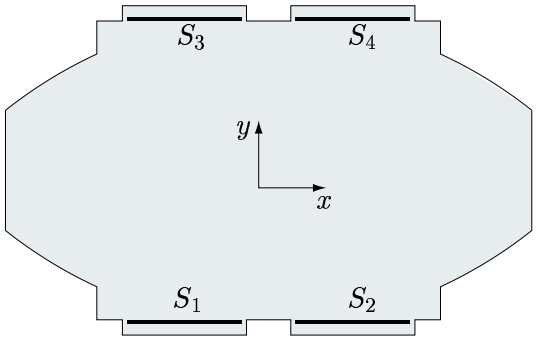

FIG. 1: Arrangement of buttons in CESR arc BPMs.

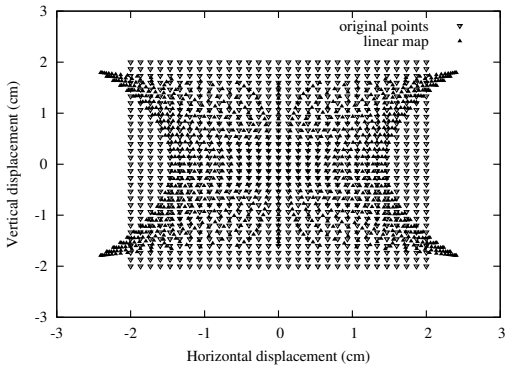

FIG. 2: Linearized map distortion in CESR arc BPM.

II. BACKGROUND

The BPMs in CESR are button-style detectors with four electrodes arranged as shown in Fig. 1. The passing bunch induces a surface charge on the button producing a voltage signal which is proportional to the distance of the beam from the electrodes. At small beam amplitudes the button response can be linearized and that is how many accelerator laboratories proceed. However this linearization method fails at large beam amplitudes which is of concern at CESR where beams in colliding conditions travel on large amplitude pretzel orbits. The failure of the linear button response model has been measured at CESR and has been named the pincushion effect for the distinct shape seen in Fig. 2. Thus the goal of the BPM studies at CESR have been focused on formulating an accurate nonlinear model of the BPM response.

A. BPM Calibration

A complication to either a linear or nonlinear BPM response model arises due to the physical differences between the BPM buttons. There are known limitations during the BPM construction process which cause differences in the depth and position of insertion of BPM buttons into the aluminum pipe wall. We assumed in this experiment that these insertion distance differences do not cause a significant change in the functional form of the fields nearby and only cause each button to have different gains. The gain coefficients for each button are labeled b_i and can be calculated from the measured coupling between button

i and j, $\tilde{U}_{ij}$, using the following equations, [2, 3]

$$b_1 = 1 \,, \tag{1}$$

$$b_2 = \sqrt{\frac{\tilde{U}_{23}\tilde{U}_{24}}{\tilde{U}_{13}\tilde{U}_{14}}} \,, \tag{2}$$

$$b_3 = \sqrt{\frac{\tilde{U}_{23}\tilde{U}_{43}}{\tilde{U}_{12}\tilde{U}_{14}}} \,, \tag{3}$$

$$b_4 = \sqrt{\frac{\tilde{U}_{24}\tilde{U}_{43}}{\tilde{U}_{12}\tilde{U}_{13}}} \,. \tag{4}$$

Calculations of these gain coefficients using measured values for the coupling between each pair of buttons has been done previously at CESR at frequencies up to 100 MHz with documented success [4, 5]. The BPM test stand described in this paper was used to investigate the frequency dependent behavior of this coupling response as well as examine different ways to extract the coupling response from the BPMs including those not involving attaching a spectrum analyzer to every button on every BPM in CESR.

B. Nonlinear Model for BPM Response

A nonlinear model for the BPM button response has been formulated and put into use at CESR by Helms and Hoffstaetter [5]. As opposed to linearizing the button response, this nonlinear model incorporates a realistic numerical model of the button response using Green's reciprocity theorem. Green's reciprocity theorem states that if we have two separate configurations of scalar potentials ϕ_1 and ϕ_2 in a volume V bounded by a surface S, then

$$\int_V \phi_1 \rho_2 \; dV + \oint_S \phi_1 \sigma_2 \; da = \int_V \phi_2 \rho_1 \; dV + \oint_S \phi_2 \sigma_1 \; da, \tag{5}$$

where σ_i and ρ_i are the surface and volume charge densities associated with ϕ_i. As described in [5], if we allow ϕ_1 to correspond to the situation when one button is at a potential V and all other surfaces are grounded, then the potential $\phi_1(x, y)$ can be calculated numerically for all (x, y) inside the beampipe. If we now let ρ_2 model an electron beam by placing a point charge q at some location (x_0, y_0), Green's reciprocity theorem can be solved to show

$$q_b = \frac{-q\phi_1(x_0, y_0)}{\mathcal{V}}, \tag{6}$$

the response at a button is proportional to the surface charge on it. Therefore the response of a button to a point charge at (x_0, y_0) is proportional to the scalar potential measured at

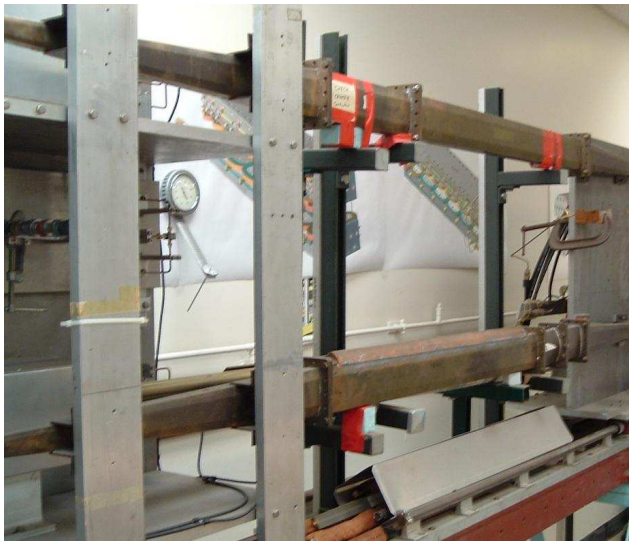

FIG. 3: The G-Machine, named for its ability to measure G the higher mode loss parameter. Plain sections of copper beampipe are mounted in the dual-arm apparatus.

that same point if there were no charge and the button was excited with some fixed potential $\mathcal{V}$. This result was used by Helms and Hoffstaetter to formulate a nonlinear model for the BPMs in CESR.

This nonlinear model has been shown to improve the measurement of large amplitude particle beams and eliminate the pincushion effect in CESR. However these results inspire limited confidence in the nonlinear model because the improvements in the BPM measurements were shown using systems which themselves depended on the BPM measurements. For example, measuring beam position versus seperator strength in CESR requires varying the separators which are themselves calibrated from BPM measurements [5]. The BPM test stand described in this paper was used to experimentally show the elimination of the pincushion effect using the nonlinear model described by Helms and Hoffstaetter in such a way that was independent of the BPM measurements.

III. THE TEST STAND

The two arm energy loss measurement apparatus which was converted into a BPM test stand is called the G-Machine and is shown in Fig. 3 and documented in reference [6]. A stationary brass rod was threaded through the copper beampipe in the original configuration of the G-Machine, and slight modifications to this apparatus allowed it to be used to study

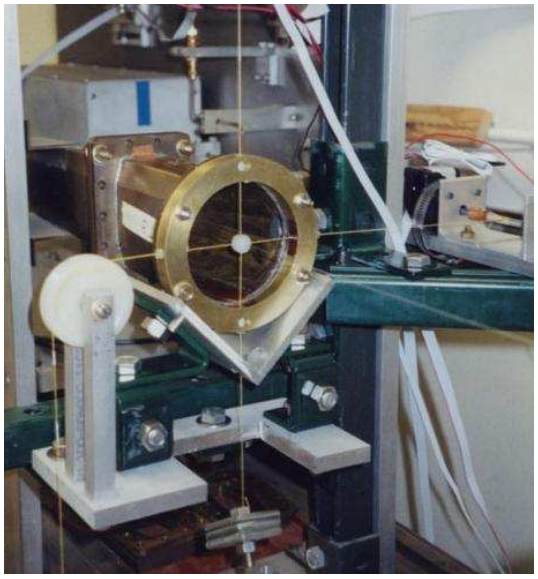

FIG. 4: Wire pulling mechanism implemented in BPM test stand.

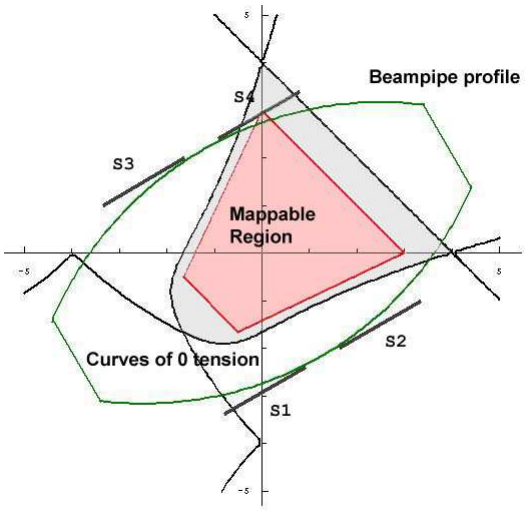

FIG. 5: Tension limitations on motion range. S_1 - S_4 show the button positions.

3 CESR arc BPMs. Replacing the copper beampipe in one of the arms of the G-Machine by sections of CESR vacuum chamber mounted with BPMs and terminating the brass rod, allowed the coupling response between buttons on the BPMs to be measured with a spectrum analyzer. After BPM characterization results were achieved with the stationary brass rod, the G-Machine was modified to support a movable wire which would allow a 2-D map of the interior of a CESR arc BPM to be performed.

The hardware construction was complicated by the fact that the movable wire needed to be supported by a small, electrically neutral structure so its presence inside the beampipe would not perturb the fields significantly. Thus, the wire was threaded through two nylon collars, one at each end of the beampipe. Each collar was supported by four Kevlar strings; Kevlar selected to minimize stretching. Two of these strings were attached to counterweights, and each of the other two strings was attached to a perpendicularly oriented lead screw assembly that provided accurate linear motion. Using stepper motors to control the lead screws, it was possible to accurately position the wire inside the BPM (Fig. 4).

However, the geometry of the setup limited the range through which the wire could be moved. The tension in both of the supporting strings is a function of the (x, y) coordinates of the wire; at certain points inside the beampipe, the tension in one of these strings goes to zero and the string becomes slack. At this point the position of the wire is no longer

well-defined, limiting the wire's range of motion. Numerically solving for the zero tension curves in each string gives Fig. 5, where the wire can only be moved through the shaded area shown; note the BPM was rotated by 60 degrees to maximize the area that could be mapped.

The reproducibility and accuracy of the setup were limited by the fact that several key components of the hardware were made out of materials (such as nylon) that deform under stress. The accuracy was tested by moving the wire through a 2-D grid and measuring the actual position of the wire using optical survey equipment. It was found that though the actual position of the wire differed from the theoretical position by up to 500 μm, the position was reproducible to within 10 μm.

It was also necessary to electrically terminate the wire at the far end of the G-Machine in a way that would allow tension to be placed on the wire to keep it tight inside the beampipe. This was done by soldering the wire to a brass rod which was then threaded through the center of a 78 Ω BPM termination resistor. A string was attached to the brass rod and then passed over a pulley so that a counterweight could be attached to the rod, keeping the wire tight inside the beampipe. However, the impedance of this terminator was not perfectly matched with that of the beampipe, leading to resonances at multiples of the frequency corresponding to the length of the beampipe.

Data from all of this BPM test stand was taken using two different Hewlett Packard spectrum analyzers, the HP3588A with a maximum frequency of 150 MHz and the HP8593 which has a maximum frequency of 2.9 GHz. Both spectrum analyzers were controlled by a Windows PC through a GPIB connection using National Instrument's LabView program. The stepper motors were MDIF1713-E models from Intelligent Motion Systems and were controlled by LabView over a serial port connection. The lead screw assemblies were pre-assembled LS6A2-6 models from WM-Berg.

IV. BPM CHARACTERIZATION RESULTS

The BPM test stand described here was used to gather data to characterize the frequency dependent behavior of the BPMs used in CESR. Data was gathered on a variety of different CESR arc BPMs in the test stand and compared with data gathered on some of the same and some different CESR arc BPMs after they were mounted in CESR. Results were gathered in

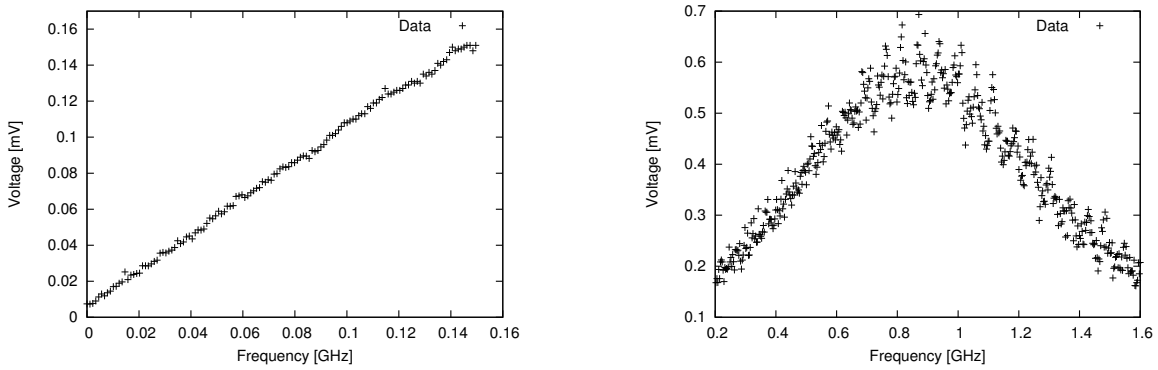

FIG. 6: BPM button-to-button coupling spectra at low & high frequencies from button 1 to 2.

TABLE I: Coupling coefficients, b_i, for one CESR arc BPM.

Button #	1	2	3	4
Coupling	1.00	0.99	1.02	0.94

an effort to more fully understand the button-to-button coupling measurements performed previously in CESR [4] and the button-to-wire response spectra as relevant to a simulated model of the BPMs [5].

A. Button Coupling

At low frequencies, it is believed that the BPM button coupling U_{ij} behaves similar to a high pass filter where R is the termination resistor attached to button j and C is the capacitive coupling from button i to button j. Fig. 6A shows that the low frequency range of the coupling spectra (button-to-button) is linear, in agreement with the high-pass filter model. Using the known button termination resistor value ($R = 80\ \Omega$) to fit the slope of the coupling spectra yields a value of $C = 0.01$ pF for the capacitive coupling. This value for the capacitive coupling makes sense as it is at least as small as the capacitance value you would calculate using a parallel plate model for the capacitive coupling between two BPM buttons. Additionally, the low frequency range of the coupling spectra and capacitive coupling result (see Table I) is equivalent to previous results for CESR arc BPMs [4].

Using a higher frequency spectrum analyzer than previous measurements [4], we examined the validity of treating the capacitive coupling as a simple high pass filter at high frequencies.

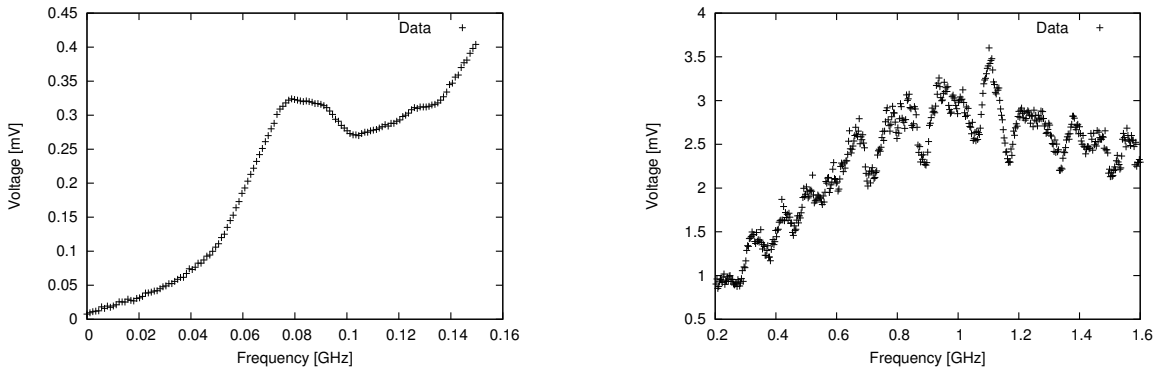

FIG. 7: BPM button-to-wire response spectra at low & high frequency for button 1, with wire at (0,0).

It can be seen in Fig. 6B that above 800 MHz the button coupling no longer appears linear. That such a high pass filter would still have a linear relationship between frequency and voltage at 800 MHz shows that our lump circuit model must be modified at higher frequencies. However we were unable to come up with a new lump circuit model to describe the shape of the data at high frequencies.

B. Button Response

Using the test stand with threaded wire, we were able to examine the response of the BPM as well (wire-to-button). The arc BPM button response to a signal on the wire at low frequency can be seen in Fig. 7A and at high frequency in Fig. 7B. Again, it is hypothesized that at low frequencies the dominant connection between the wire and the button is a capacitive coupling and can thus be treated as a high-pass filter with a linear relationship between voltage and frequency. Fig. 7A is not obviously linear, however Fig. 7B does show a linearly increasing trend in the voltage up to nearly 1 GHz. Thus the high-pass filter model was deemed adequate and the slope of the frequency response was taken to represent the signal strength, as in the capacitive coupling case.

We tried to describe the high frequency dependence of the BPM button response to a voltage simulating a particle beam in terms of lump circuit elements as can be done for the button coupling at low frequencies. However, attempts to explain the shapes of this data using lump circuit elements were unsuccessful. Unfortunately, the response of CESR BPMs

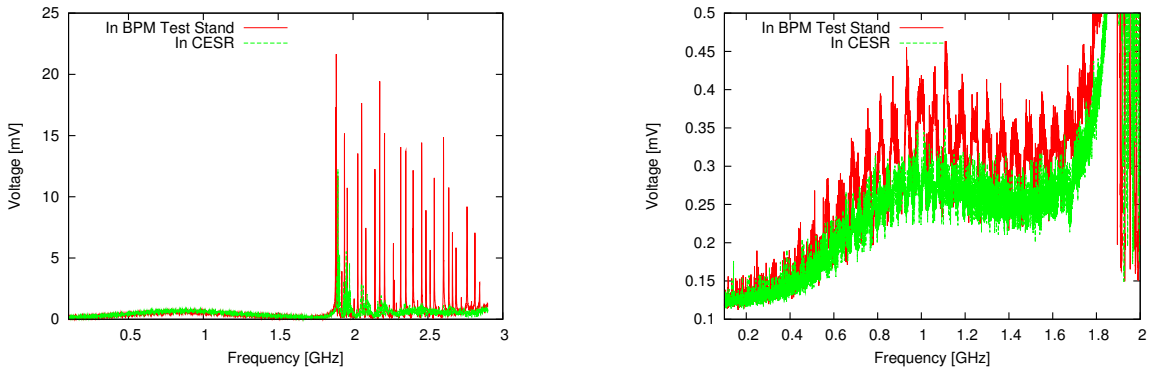

FIG. 8: BPM button 1-to-4 coupling spectra. Data taken on BPM in test stand and in CESR.

to a real particle bunch peaks around 750 MHz, so understanding the behavior of the data in this region where the high pass filter model is breaking down is critical to a complete model of CESR BPM response. The work documented here is being followed-up on with on-going simulation efforts to understand the BPM button response behavior.

C. Other Experimental Features

As can be seen in Fig. 8A, above about 1.8 GHz the button-to-button spectra shows chaotic resonances, the same is found with button-to-wire spectra. The cutoff frequency of the TE_{10} mode for a rectangular waveguide with the same width as the major axis of the beampipe is 1.66 GHz. It is thought that as we exceed this frequency, TE and TM modes can propagate down the beampipe and disturb our measurements. The same type of high frequency resonances are seen in the button-to-button measurements preformed on the BPMs installed in CESR. This supports the hypothesis that the resonances comes from the beam pipe. Because of this, no results were produced using the data above 1.8 GHz.

There is also a higher frequency interference effect superimposed on the data, Fig. 8B, with peaks occurring approximately every 100 MHz. This is the right spacing to be caused by a resonance effect due to imperfect termination of the wire at the end of the beampipe. It corresponds roughly to the second fundamental mode of vibration of the whole beampipe at 116 MHz. That the interference effect was not seen in the coupling spectra measured on the BPMs in CESR says that this is a characteristic of the sealed ends of the test stand. Since this aspect of the spectra is not a feature of the BPMs themselves, later results were

taken by averaging over these high frequency oscillations.

Finally, results for the capacitive coupling between the buttons were desired which could cross-check, as well as speed up, the spectrum analyzer method described above to measure the b_i's. An experiment was performed which used a stationary rod mounted in a section of CESR beam pipe with three arc BPMs on it. The BPM response to a low frequency signal on the stationary rod was measured from which the rod position was calculated. Additionally, the rod's transverse position at the longitudinal position of the three BPMs was measured with optical survey equipment aimed down the beam pipe. This beam pipe was later mounted in CESR so keeping the interior of the pipe clean and unblemished was critical. Unfortunately, no reliable result was achieved from this experiment due to the errors and physical limitations in the hardware setup, the difficulty of measuring the rod position in such a restrictive geometry, and the inability to accurately fix the position of the rod in a clean environment.

V. BPM MAP RESULTS

The movable wire test stand was used to translate the wire over a large region of the interior of a CESR arc BPM while at the same time reading the BPM button-to-wire response with a spectrum analyzer. As described above, the slope of the frequency response was taken to represent the signal strength at each point. On the low frequency data (up to 150 MHz) the slope was taken from 50 to 70 MHz, and on the high frequency data the slope was taken from 0 to about 700 MHz. Both the low frequency experimental map and the high frequency experimental map were used to test the simulated nonlinear map of the BPM response generated by Helms and Hoffstaetter.

A. 1-D Scan, Original Hardware

To eliminate possible errors which might be introduced by the horizontal and vertical motors pulling on the wire at the same time, the first experimental map of the BPM response was performed with just the horizontal motor in a 1-dimensional slice with the movable wire centered in the BPM as seen in Fig. 9. However this scan was performed with the movable wire using an original version of the hardware setup, before the lead screw assemblies were

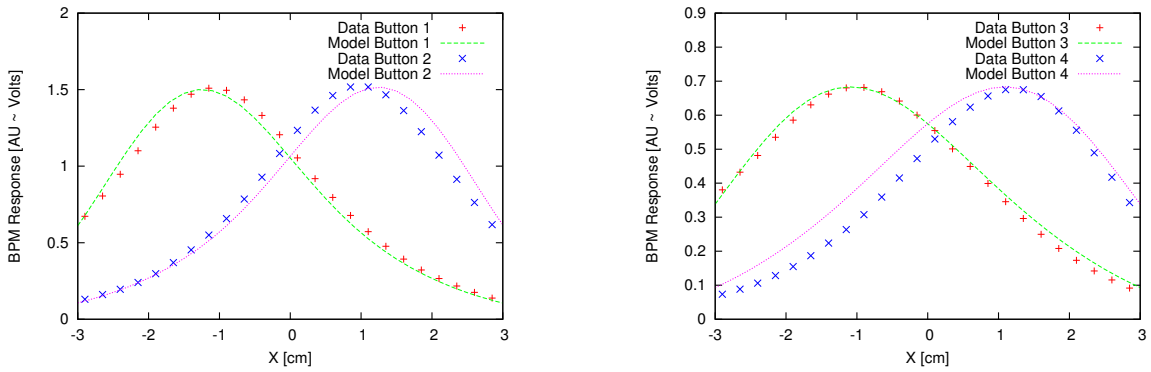

FIG. 9: 1D scan of BPM interior through y = -6mm from button 1 & 2 (left) and 3 & 4 (right). The points are the data (shifted by x = -6mm) and the curves are the simulated model.

installed which achieved the 500 μm absolute position and 10 μm reproducibility. The limitations to the original hardware produced an error in the positioning of the wire so that when the wire was intended to be positioned in the center of the BPM, in fact the experimental data agrees best, both in shape and in relative gain between buttons 1,2 and buttons 3,4, with the model through y = -6mm. Additionally, errors in the hardware produced a x = 6mm horizontal offset in the collected data. Despite the imprecise position of the wire in this experiment, the model agrees well taking these offsets into account and this initial result was used to motivate an upgrade to the hardware to provide the needed accuracy in position to perform a 2-D scan of the BPM.

B. 2-D Scan, Upgraded Hardware

Using the upgraded harware system with the lead screw assemblies and improved positioning and reproducibility, a 2-D scan of the entire interior of the BPM was performed. A comparison between the experimental and simulated map of the BPM interior can be seen in Fig. 10 and Fig. 11.

For all four buttons, good agreement exists between the experimental and simulated 2-D maps, both in the low frequency and high frequency regimes (not shown). The RMS residual for each button relative to the peak signal strength is listed in Table II. The agreement is the best for buttons 1, 2 and 3, where the wire remains far from the button on which the signal is being measured. As can be seen in more detail in the contour error plots in Fig. 12

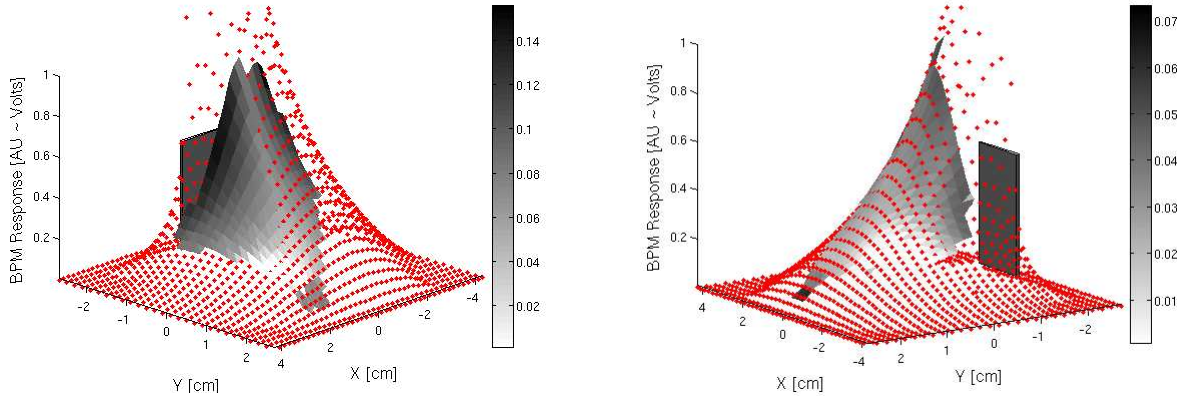

FIG. 10: 2D scan of BPM interior from button 1 (left) & 2 (right). The points are the simulated model, surface is the experimental data, intensity is the error, and the rectangle shows button position.

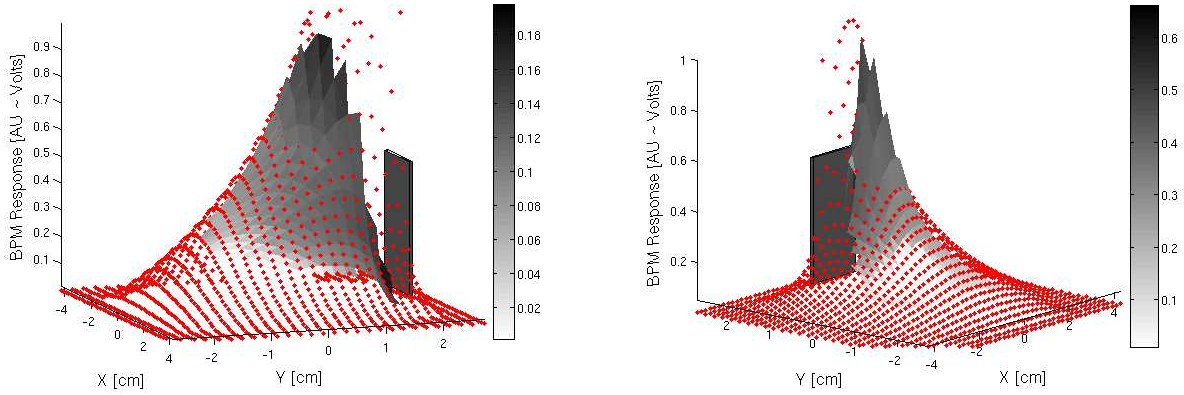

FIG. 11: 2D scan of BPM interior from button 3 (left) & 4 (right). The points are the simulated model, surface is the experimental data, intensity is the absolute error, and the rectangle shows button position.

and Fig. 13, the magnitude of the error increases when the wire comes close to the button.

TABLE II: RMS value of absolute error between experimental and simulated 2-D maps.

Button #	1	2	3	4
RMS Error	5.0%	1.8%	5.5%	14.6%

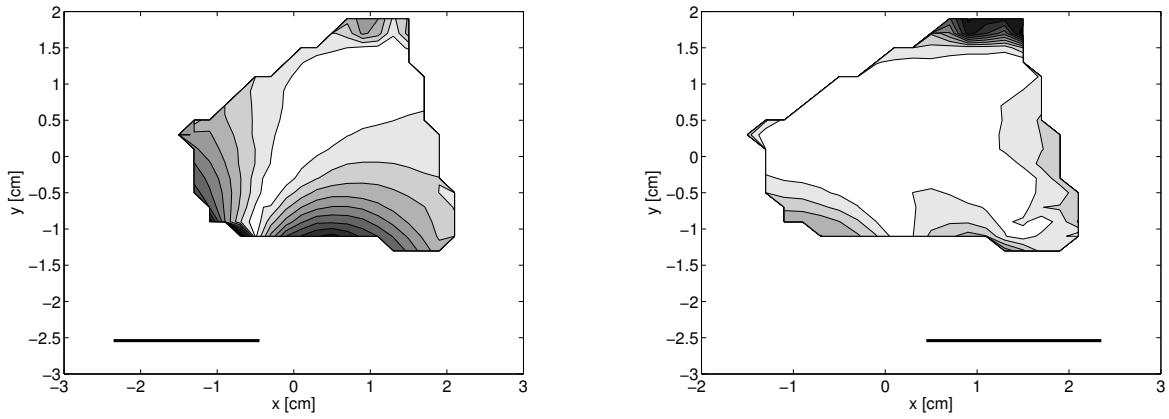

FIG. 12: Contour of residual between experimental and simulated 2-D maps for button 1 (left) & 2 (right). See Fig. 10A & B for intensity scales.

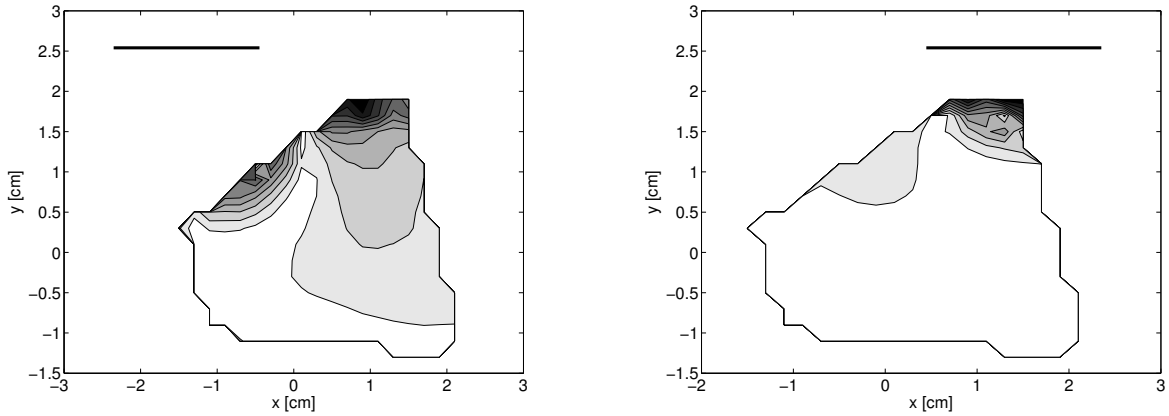

FIG. 13: Contour of residual between experimental and simulated 2-D maps for button 3 (left) & 4 (right). See Fig. 11A & B for intensity scales.

C. Interpretation of Results

We know that inaccuracies in the BPM manufacturing process cause variations in the insertion distance of the buttons into the BPM aluminum wall. We assumed previously that this would only cause gain differences between the buttons, i.e. there would be no difference in the functional form of the signal measured at each button. From Eq. 6, this means that we assume that the potential function $\phi_i(x, y)$ changes only by a scalar multiple if we vary the insertion distance of the button in the beampipe wall. While this is a reasonable assumption when (x, y) is far from the position of the button itself, it seems that close to the

TABLE III: Data to model scaling coefficients, normalized to button 1.

Button #	**1-D Low Freq**	**2-D Low Freq**	**2-D High Freq**
1	1.00	1.00	1.00
2	1.01	1.20	1.10
3	0.70	0.63	0.66
4	0.54	0.55	0.74

button, any change in the insertion distance would have a more complicated effect on the functional form of $\phi_i(x, y)$. This means that our approximation becomes less valid when we move the wire close to the button, explaining the position-dependence of the error between our experimental and simulated nonlinear models.

We were somewhat less successful explaining an effect which concerns the relative magnitudes of the signal strengths from each of the buttons. The experimental data was normalized to fit the theoretical mapping, but the normalization factor that results in the best fit differed significantly from one button the next, Table III. If there were very different capacitive couplings between the buttons then the button gains would have such varied values, however the button coupling coefficients should reflect this difference and Table I does not. We hypothesize that the coupling from wire to button does not follow the simple linear model that was used in calculating the button-to-button coupling coefficients, and a more complicated model must be used to explain this. It would be instructive to compare these with beam-based measurements of the relative button gains to see if there is a similar effect.

VI. CONCLUSIONS

The agreement between the simulated and experimental BPM mappings makes it clear that the model being used to simulate the BPM response is an accurate representation of the actual system. However, our inability to explain the different scaling coefficients indicates that more work must be done before we have a complete understanding of the CESR arc BPMs. Descriptions of the BPM response and coupling would be simplified with lump-circuit models representing the system valid over all frequencies, this behavior is not yet fully understood but is being investigated more through an on-going simulation effort by

one of the authors (M. Billing).

Future work would be desirable to extend the experiment to include higher frequencies corresponding to the small bunch lengths that will be used in the ERL. To do this, it will be necessary to use a different setup with a smaller beampipe diameter to push the resonance effects beyond a few GHz.

VII. ACKNOWLEDGMENTS

The authors would like to thank all of those that offered their time and assistance to the successful completion of this project. Andy Schwarzkopf and Christopher Chan deserve great thanks for all of the work they did in the initial stages of this project which laid the groundwork for the results the authors achieved. The authors would also like to offer their appreciation for the help provided by Harold Barnard, Scott Chapman, Gerry Codner, Chris Cooper, Rich Helms, Matthias Liepe, Jim Sexton, and Charlie Strohman.

---

[1] W. Zhou, Y. Chen, K. Ye, W. Cheng, and Y. Yang, "The Calibration of SSRF BPM", proceedings of the Second Asian Particle Accelerator Conference, 2001.

[2] G. Lambertson, "Calibration of Position Electrodes Using External Measurements", LSAP Note-5, 1987.

[3] J. Keil, "Messung, Korrektur und Analyse der Gleichgewichtsbahn an der Elektronen-Stretcher-Anlage ELS", Ph. D. Thesis, Universty Bonn, 2000.

[4] B. Meredith, "Pick-up Calibration in CESR BPMs", LEPP REU Report, 2003.

[5] R. Helms, G. Hoffstaetter, "Orbit and Optics Improvement by Evaluating the Nonlinear BPM Response in CESR", ARXIV, 2004.

[6] M. Billing, J. Kirchgessner, and R. Sundelin, "Simulation Measurement of Bunch Excited Fields and Energy Loss in Vacuum Chamber Components and Cavities", IEEE Transactions of Nuclear Science, NS-26, No. 3, 1979.